

Electrodichroism and paraelectric alignment of $\langle 110 \rangle$ -oriented OH^- centers in KI

Siegmar Kapghan* and Fritz Lüty

Physics Department, University of Utah, Salt Lake City, Utah 84112

(Received 22 December 1981)

The uv absorption of OH^- centers in KI has been studied at low temperatures under applied fields of various symmetries and in different polarization geometries. The field-induced absorption changes do not follow the spectral shape of the OH^- band and depend drastically on field and polarization geometries. This complex behavior can be accounted for by a model involving field alignment of $\langle 110 \rangle$ -oriented dipoles which are characterized by three different spectrally partially overlapping uv transitions, one polarized parallel and two polarized along the two inequivalent directions perpendicular to the $\langle 110 \rangle$ dipole axis. Strength and spectral shape of these transitions can be determined from saturation alignment experiments under $\langle 110 \rangle$ fields. With these optical parameters, the measured electro-optical behavior can be fitted rather well to a simple paraelectric model, yielding for the only free-fitting parameter an uncorrected (for local fields) electric dipole moment of $1.35 \pm 0.1 e \text{ \AA}$.

I. INTRODUCTION

Among the various experimental techniques used to study field alignment of OH^- defects in alkali halides, electro-dichroism measurements of the ultraviolet OH^- absorption have been very prominent and successful and have in fact initiated the whole field of paraelectric defect investigation with the $\text{KCl}:\text{OH}^-$ system.¹ These field-induced absorption changes $\Delta K(\omega, \vec{E}, T)$ for $\text{KCl}:\text{OH}^-$ (measured with light polarization perpendicular to the applied field \vec{E}) were found to be highly anisotropic (strongest effect for $\langle 100 \rangle$ fields), display an initial $(E/T)^2$ dependence, and follow in their spectral shape $\Delta K(\omega)$ the original absorption band $K(\omega)$. Extension of these measurements to a large number of hosts² showed essentially the same electro-dichroism properties of OH^- in KBr , RbCl , RbBr , and RbI . This behavior could be explained in terms of a paraelectric alignment model for $\langle 100 \rangle$ -oriented permanent electric dipoles of electric moment p , characterized optically by a single field-independent absorption transition $K(\omega)$, which has different oscillator strength f for light polarization parallel (\parallel) and perpendicular (\perp) to the molecular axis. Evidently this model of electrically and optically permanent dipoles leads to only zero-moment absorption changes [i.e., $\Delta K(\omega, E, T) = A(E, T)K(\omega)$] under dipole alignment, as experimentally observed. In all the above-mentioned

host crystals, the polarization anisotropy of the optical transition $g \equiv f_{\parallel}/f_{\perp}$ was found to be rather constant with $g = 0.3 \pm 0.04$. No explanation could so far be given for this peculiar anisotropic absorption behavior of the OH^- defect, in spite of theoretical attempts.³ Electrocaloric measurements on several of the above-mentioned systems² confirmed independently the $\langle 100 \rangle$ dipole model.

In KI host material the OH^- defects behave very differently. Electrocaloric measurements showed the largest effect for $\langle 110 \rangle$ fields,² indicating dipole orientation in (or at least close to) $\langle 110 \rangle$ crystallographic directions. This was supported by ir measurements of the OH^- librational absorption.⁴ Extended paraelectric resonance studies revealed a very complex double multiplet behavior of the $\text{KI}:\text{OH}^-$ system,^{5,6} which—at least in its essential features—could again be best explained in terms of a $\langle 110 \rangle$ dipole model.⁷

Our first preliminary electro-optical^{2,8} as well as elasto-optical⁹ measurements yielded puzzling results quite different from the ones obtained for other OH^- systems, showing highly anisotropic $\Delta \vec{K}(\omega, E, T)$ effects which do not follow the spectral shape $K(\omega)$ of the absorption. As only measurements with light polarization perpendicular to the applied field were available at that time, no conclusive model could be derived.

In this work we present and analyze the results of a comprehensive study of the uv electrodi-

chroism of the KI:OH^- system, which includes all absorption changes $\Delta K(E, \omega)$ measured for light polarization parallel and perpendicular to the applied field. Most of the experiments were performed at temperatures below 2 K in order to reach full alignment saturation, necessary for accurate analysis of the OH^- optical anisotropy.

II. EXPERIMENTAL TECHNIQUES

The crystals were grown at the crystal growth laboratory of the University of Utah by the Kyropoulos method, using ultrapure (Merck u.p.) material. Controlled amounts of KOH were added to the melt $[(0.5-5) \times 10^{-3} \text{ mol ratio}]$ under an argon atmosphere. The OH^- concentration in the crystal $(2 \times 10^{17} - 3 \times 10^{18} n_{\text{OH}}/\text{cm}^3)$ was determined from the uv absorption band using the oscillator strength ($f=0.06$) based upon earlier chemical pH analysis.²

The measurements were performed in an optical helium cryostat which permitted the application of an electric field with transparent nickel nets (40- μm mesh width embedded in an indium-covered frame) either parallel or perpendicular to the propagation of the light beam (\vec{k}). The temperature was measured directly at the sample with a calibrated thermistor ($\frac{1}{8}$ Watt Allen-Bradly 100- Ω resistor) in good thermal contact to the crystal surface at the side of the ground electrode. Properly oriented samples were cut and polished with typical dimensions $20 \times 20 \text{ mm}^2$ with a thickness of 0.1–1 mm for $\vec{k} \parallel \vec{E}$ and with dimensions $20 \times 5 \text{ mm}^2$ with a thickness of 2–3 mm for $\vec{k} \perp \vec{E}$.

The OH^- -induced uv absorption was measured in a Cary 14 and 17 spectrometer by comparing the transmission of the doped sample with that of a pure host crystal at the same temperature. The linear polarization of the light was obtained using an air spaced, uv-grade Glan-Thomson prism polarizer.

III. EXPERIMENTAL RESULTS

OH^- ions in KI give rise to an uv absorption band at about 5.3 eV accompanied by a strong absorption increase on the high-energy side of this band.² Application of an electric field at low temperatures induces changes of the uv absorption band, which in their spectral shape deviate considerably from the original OH^- absorption band. The spectral form and the integrated area under

the absorption curve depend on temperature, applied field (and its direction), and on the polarization of the light.

The spectra have been plotted only up to 5.6 eV because at higher energies the fundamental absorption of the crystals and the absorption of the polarizers combine to yield a very steep increase of the absorption, which makes a precise determination of the relative field-induced changes very difficult.

Figure 1 shows the OH^- absorption band and the field-induced absorption changes for fields applied in $\langle 100 \rangle$ and $\langle 111 \rangle$ direction. In these cases the integrated absorption for light polarized perpendicular to E increases while decreasing for light polarized parallel to E . None of these changes $\Delta K(\omega)$ follows the original absorption band $K(\omega)$. Figure 2 shows the induced absorption changes under $\langle 110 \rangle$ fields. For $\vec{k} \parallel \vec{E}$ and unpolarized light (i.e., light with its E vector in the plane perpendicular to the applied field E_{110}) the observed absorption increase $\Delta K(\omega)$ follows spectrally the absorption-band shape $K(\omega)$. This absorption increase, however, consists of a superposition of two spectrally different components, as measurements with light polarized along the two symmetry-inequivalent directions perpendicular to the E_{110} field (001 and $1\bar{1}0$) (see Fig. 2) clearly reveal. For light polarization parallel to E_{110} a strong $\Delta K(\omega)$ decrease is observed which follows spectrally the OH^- absorption band $K(\omega)$.

From these measurements, the ratio of the zeroth moment or integrated absorption (between 5.0 and 5.6 eV) $\langle K(E) \rangle^0 : \langle K(0) \rangle^0$ can be easily obtained. The results are plotted (in an E/T scale) for E_{111} and E_{100} in Fig. 3, and for E_{110} in Fig. 4. Qualitative inspection shows that the integrated absorption $\langle K(E) \rangle^0$ under all values and directions of the field, when averaged over the three light-polarization directions (one parallel and two perpendicular to E) always yields the original value $\langle K(0) \rangle^0$. In other words, field application does not change the total integrated absorption of the OH^- system but only distributes them in different ways among the polarization directions parallel and perpendicular to E .

From the results in Figs. 1–4, some qualitative conclusions can be drawn immediately:

(1) If a simple dipole reorientation model can be applied, it has to be a $\langle 110 \rangle$ dipole model since only for this equilibrium direction a strong ΔK effect for all the field directions ($\langle 100 \rangle$, $\langle 111 \rangle$, and $\langle 110 \rangle$) can be expected. For a possible $\langle 100 \rangle$ and $\langle 111 \rangle$ dipole model the application of $\langle 111 \rangle$ or

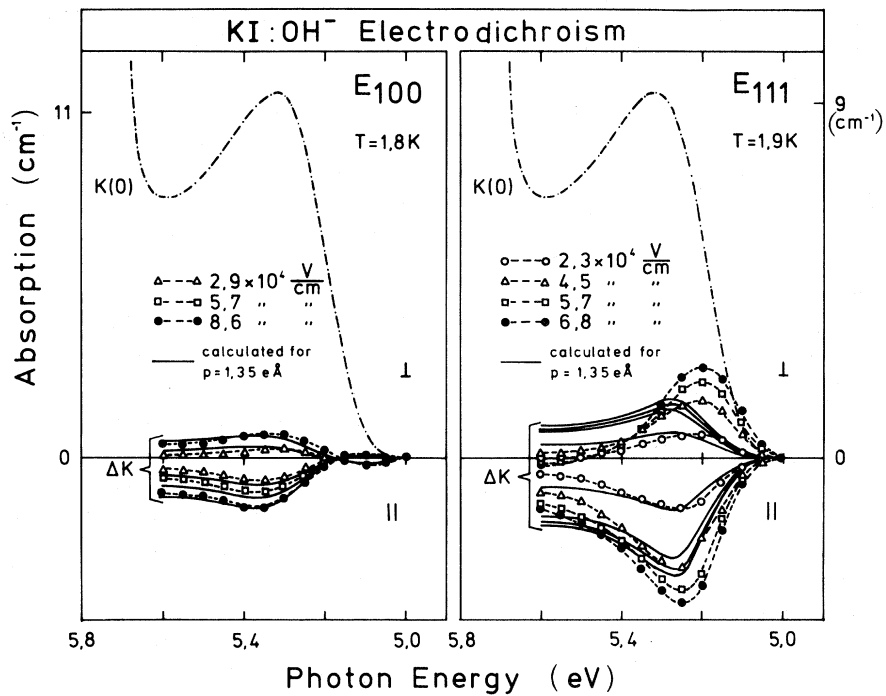


FIG. 1. Field-induced absorption change of the OH^- band in KI at $T \sim 2$ K, for light polarized parallel (||) and perpendicular (\perp) to an applied E_{100} and E_{111} field.

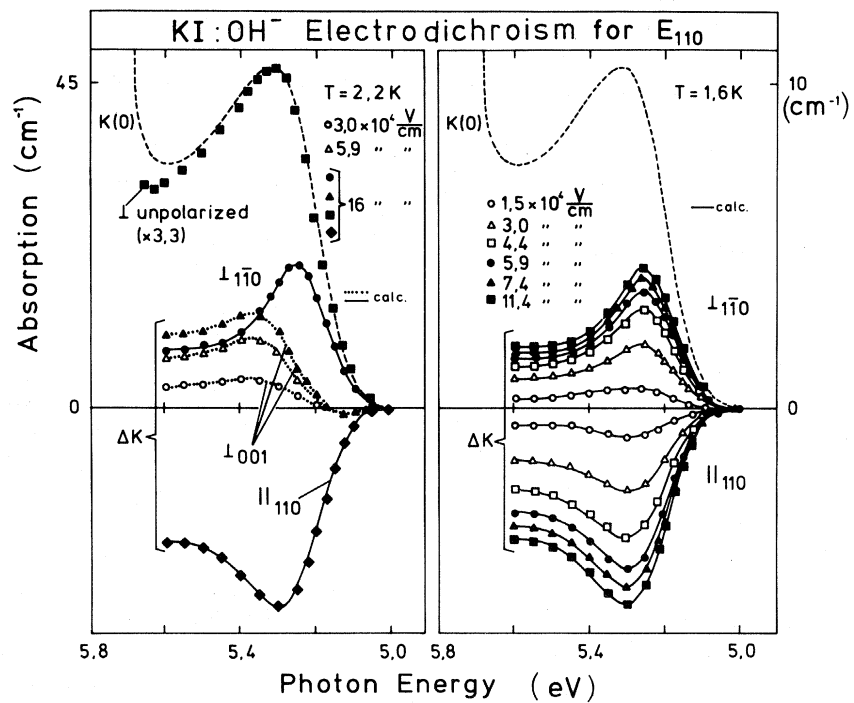


FIG. 2. Field-induced absorption change of the OH^- band in KI for light polarized parallel and perpendicular to an applied E_{110} field.

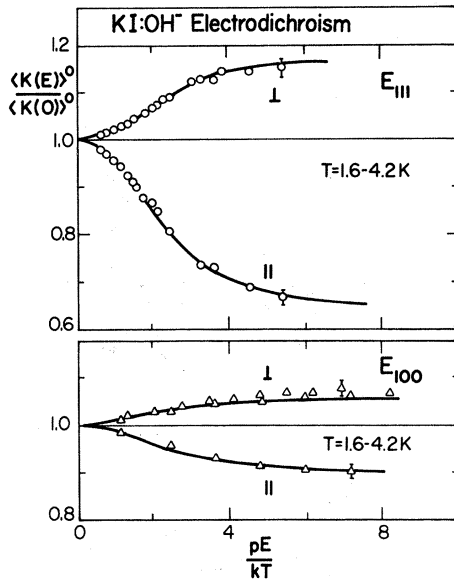


FIG. 3. Relative integrated absorption (5.0–5.6 eV) for light polarized parallel and perpendicular to an electric field applied in the [111] and [100] direction. The full curve has been calculated using $p = 1.35e \text{ \AA}$ and the optical anisotropy model described in the text.

$\langle 100 \rangle$ fields, respectively, should not produce any reorientation dichroism.

(2) The observed absorption increase for light polarized perpendicular and the absorption decrease for light polarized parallel to the applied field indicates an optical transition moment mainly perpendicular to the dipole axis (π polarization).

(3) π -polarized transitions alone, however, are not sufficient to explain the observed behavior. Even under highest E/T values and saturated absorption changes (i.e., full dipole alignment) a small amount of optical absorption polarized parallel to E remains. If a $\langle 110 \rangle$ dipole model is correct, saturation alignment under E_{110} fields should display quantitatively the full optical anisotropy of the OH^- center.

IV. MODEL FOR $\langle 110 \rangle$ DIPOLE SYSTEM AND ITS ELECTRODICHROISM

For a quantitative interpretation we want to make use of the $\langle 110 \rangle$ dipole model illustrated in Fig. 5, successfully applied before¹⁰ to explain the electro-optical behavior of another $\langle 110 \rangle$ -oriented dipole system, off-center Ag^+ defects in RbCl and RbBr . For one selected dipole site out of the

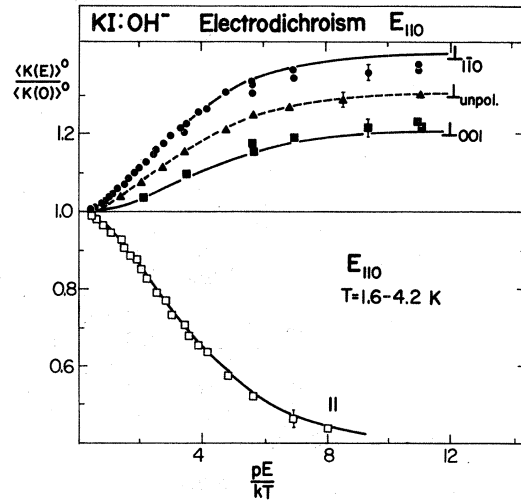


FIG. 4. Relative integrated absorption for light polarized parallel and perpendicular to the electric field applied in [110] direction. The full curve has been calculated using $p = 1.35e \text{ \AA}$ and the model described in the text.

twelve possible $\langle 110 \rangle$ orientations (site No. 3 in Fig. 5), there are in C_{2v} symmetry three different optical-dipole transition moments possible, one polarized parallel to the molecular axis (σ_{110}) and one each along the two inequivalent directions perpendicular to the dipole (π_{001} and $\pi_{1\bar{1}0}$). Each of these three transitions can give rise to an absorption band, different in strength and spectral shape, which we will call $K_1(\omega)$ for σ_{110} , $K_2(\omega)$ for $\pi_{1\bar{1}0}$, and $K_3(\omega)$ for π_{001} . The linear superposition of these three bands creates the inhomogeneously broadened band shape of the defect $K(\omega)$; i.e.,

$$K(\omega) = [K_1(\omega) + K_2(\omega) + K_3(\omega)] .$$

Under field-induced dipole reorientation, the transition moments of these three linearly polarized absorptions will rotate "rigidly" with the dipole molecule, creating the electrochromism absorption changes. For a $\langle 110 \rangle$ dipole model under full saturation E_{110} alignment, the optical absorptions measured \parallel , $\perp_{1\bar{1}0}$, and \perp_{001} to the electric field should therefore directly display the three transitions K_1 , K_2 , and K_3 . Using the saturation measurements from Fig. 2, we can therefore experimentally construct and plot the three spectral curves $K_1(\omega)$, $K_2(\omega)$, and $K_3(\omega)$ (pointed lines in Figs. 6 and 7), the superposition of which yields the original OH^- absorption band $K(\omega)$ (dotted line in Fig. 6).

Using the level splitting and multiplicity for

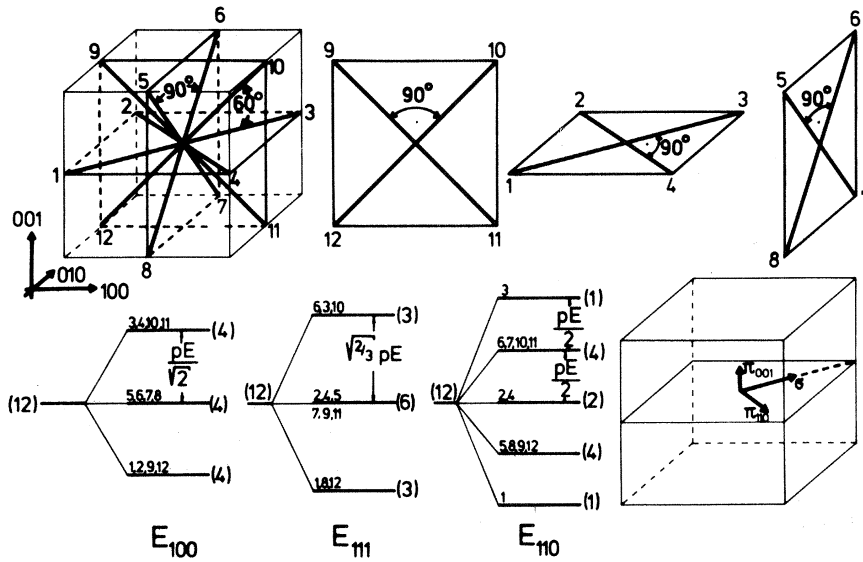


FIG. 5. $\langle 110 \rangle$ dipole model with illustration of the 12 equivalent sites and the two types (60° and 90°) of reorientation processes. The lower part shows the level splitting under field and for a selected localized dipole state (No. 3) the direction of the transition moments for the optical absorption.

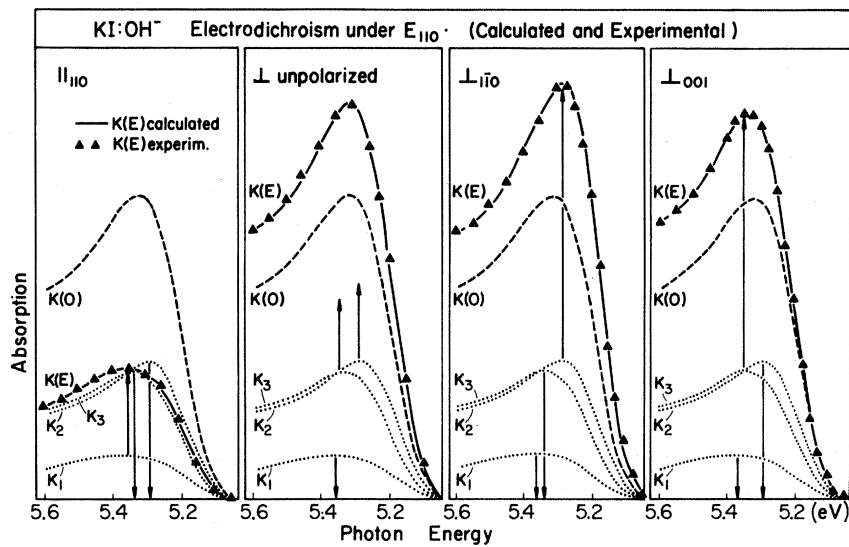


FIG. 6. Measured $K(E)$ spectra (triangles) for E_{110} in parallel and perpendicular polarizations for highest achieved E/T values in comparison to the OH^- absorption band $K(0)$ and its three subcomponents K_1 , K_2 , and K_3 . For the latter, the arrows indicate the expected changes in strength under saturation field alignment, resulting in a calculated $K(E)$ saturation spectrum given by the full line.

$\langle 110 \rangle$ paraelectric dipole model (Fig. 5), it is easy to derive with Boltzmann statistics the quantitative relations for the field-induced absorption changes expected for light polarized parallel and perpendicular to fields of different symmetries. These relations, expressed in terms of the three absorption components K_1 , K_2 , and K_3 , are summarized in Table I. For calculation of the *integrated absorption changes*, the spectral shape of the three components is irrelevant and only their *relative strength* counts. Experimentally we find for the relative strength of the three components $K_1:K_2:K_3$ a ratio 15:44:41 [percent of the total absorption $K(0)$]. The integrated absorption behavior under field, calculated with this strength ratio, can be compared to the experimentally measured one, leaving as the only open fitting parameter the dipole moment p . As Figs. 3 and 4 show, a perfect fit between calculated and measured behavior for all field and polarization geometries can be obtained with a single fitting parameter, an (uncorrected) dipole moment value of $p = 1.35 \pm 0.1e \text{ \AA}$.

In order to determine the expected *spectral behavior*, we illustrate in Figs. 6 and 7 by arrows how the three absorption bands K_1 , K_2 , and K_3 will be changed in magnitude under dipole saturation alignment in the various field and polarization geometries. The resulting (graphically constructed) saturation absorption spectrum $K(E)$ (solid lines) are compared in Figs. 6 and 7 to the experimentally measured behavior (triangles). By definition the fit is perfect for E_{110} , because the model was designed from the E_{110} saturation experiment. A very good fit, however, is obtained for E_{100} also. For E_{111} the gross features are well given by the model, but sizable spectral deviations appear particularly in the perpendicular polarization geometry. The model can be used similarly to calculate for all measured field values and directions, the spectral $\Delta K(\omega)$ curves, and to compare them (solid lines) to the measured values in Figs. 1 and 2. We again obtain a perfect fit to the E_{110} data, a very good fit to the E_{100} data, but sizable spectral deviations in the E_{111} case, particularly at higher fields.

We have so far characterized the optical properties and anisotropy of the defect within the *molecular coordinate system* by three optical-absorption components K_1 , K_2 , and K_3 . Alternatively, we can express the optical defect-anisotropy in the framework of the *crystal symmetry* by particular (normalized) linear combinations of these three absorption transitions,

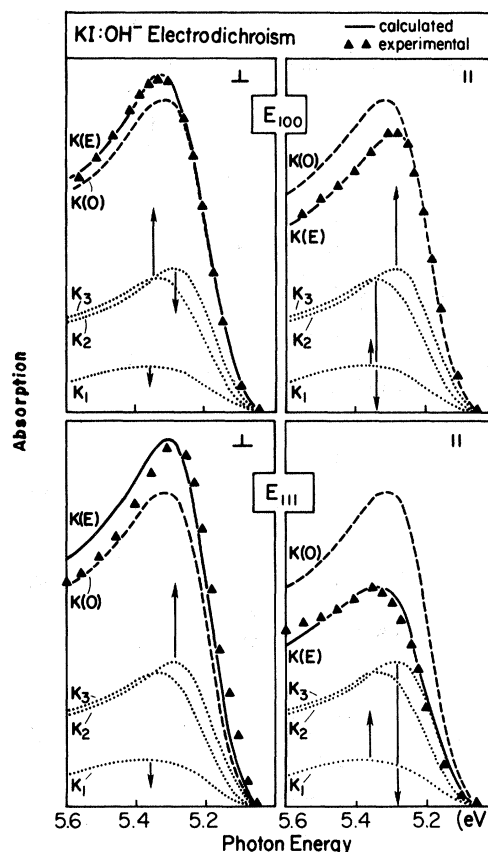


FIG. 7. Same as Fig. 6 but for E_{100} and E_{111} .

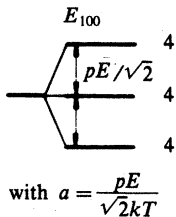
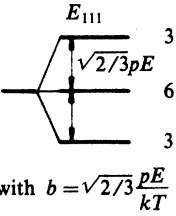
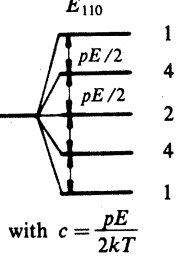
$$\Delta K(E_g) = \frac{[(K_1 + K_2)/2] - K_3}{K_1 + K_2 + K_3},$$

$$\Delta K(T_{2g}) = \frac{K_1 - K_2}{K_1 + K_2 + K_3}.$$

The first expression gives the absorption anisotropy in terms of its tetragonal (E_g) component, the second one in terms of its trigonal (T_{2g}) part. This is completely equivalent to the characterization of the elastic dipole tensor¹¹ or optical polarizability tensor¹² in terms of their E_g and T_{2g} components. Magnitude and spectral dependence of the electrochromism $\Delta K(\vec{E}, \omega)$ is determined for $\langle 100 \rangle$ fields by $\Delta K(E_g)$ only, for $\langle 111 \rangle$ fields by $\Delta K(T_{2g})$ only, and for $\langle 110 \rangle$ fields by both E_g and T_{2g} components (see Table I).

Figure 8(a) illustrates magnitude and spectral shape of these $\Delta K(E_g)$ and $\Delta K(T_{2g})$ functions in proper relation to the K_1 , K_2 , and K_3 transitions and their composite, the OH^- absorption band $K(\omega)$. It is instructive to compare this situation with the one for "normal" $\langle 100 \rangle$ -oriented OH^- centers, as derived from earlier electro- and elasto-

TABLE I. $\langle 100 \rangle$ dipole model for OH^- in KI.

Energy-level splitting	Light polarization	Absorption $K(E)$	Absorption $K(E \rightarrow \infty)$
(12)  with $a = \frac{pE}{\sqrt{2}kT}$		$\frac{4K_3 + 2(K_1 + K_2)(e^a + e^{-a})}{4(e^a + e^{-a} + 1)}$	$\frac{K_1 + K_2}{2}$
	⊥	$\frac{2(K_1 + K_2) + (K_1 + K_2 + 2K_3)(e^a + e^{-a})}{4(e^a + e^{-a} + 1)}$	$\frac{K_1 + K_2 + 2K_3}{4}$
(12)  with $b = \sqrt{2/3} \frac{pE}{kT}$		$\frac{4K_2 + 2K_3 + (2K_1 + K_3)(e^b + e^{-b})}{3(e^b + e^{-b} + 2)}$	$\frac{2K_1 + K_3}{3}$
	⊥	$\frac{3K_1 + K_2 + 2K_3 + (\frac{1}{2}K_1 + \frac{3}{2}K_2 + K_3)(e^b + e^{-b})}{3(e^b + e^{-b} + 2)}$	$\frac{K_1 + 3K_2 + 2K_3}{6}$
(12)  with $c = \frac{pE}{2kT}$		$\frac{2K_2 + K_1(e^{2c} + e^{-2c}) + (K_1 + K_2 + 2K_3)(e^c + e^{-c})}{e^{2c} + e^{-2c} + 4(e^c + e^{-c}) + 2}$	K_1
	⊥ ₁₁₀	$\frac{2K_1 + K_2(e^{2c} + e^{-2c}) + (K_1 + K_2 + 2K_3)(e^c + e^{-c})}{e^{2c} + e^{-2c} + 4(e^c + e^{-c}) + 2}$	K_2
	⊥ ₀₀₁	$\frac{2K_3 + K_3(e^{2c} + e^{-2c}) + 2(K_1 + K_2)(e^c + e^{-c})}{e^{2c} + e^{-2c} + 4(e^c + e^{-c}) + 2}$	K_3
		$K_1 \hat{=} K_{110}$	
		$K_2 \hat{=} K_{1\bar{1}0}$	
		$K_3 \hat{=} K_{001}$	

optical work [Fig. 8(b)]. The two transitions perpendicular to the molecule axis K_2 and K_3 are equal for $\langle 100 \rangle$ dipole symmetry; the parallel (K_1) transition was found to have the same spectral shape as K_2 but to be reduced in strength by a factor $g = K_1/K_2 \approx 0.3$. A large optical anisotropy

$$\Delta K(E_g) = \frac{K_1 - K_2}{K_1 + 2K_2}$$

results, while

$$\Delta K(T_{2g}) \propto K_2 - K_3 = 0.$$

Figure 8 illustrates both the similarities and differences of the two systems: The optical anisotropy *relative to the molecular axis* is very similar: In both cases we have a strong perpendicular (π) polarized transition and a spectrally very similar but about a factor of 3 smaller parallel (σ) transition. The only slight difference is the small splitting of the π transition into two spectral components for the $\langle 110 \rangle$ dipole as expected in C_{2v} symmetry. We must conclude that the essential features of the uv absorption transition and its

TABLE I. (Continued.)

Absorption change $\Delta K(E)$	Absorption change in saturation $\Delta K(E \rightarrow \infty)$
$-\Delta K_{Eg} \frac{[2-(e^a+e^{-a})]}{e^a+e^{-a}+1}$	ΔK_{Eg}
$+\frac{\Delta K_{Eg}}{2} \frac{[2-(e^a+e^{-a})]}{e^a+e^{-a}+1}$	$-\frac{\Delta K_{Eg}}{2}$
$-\Delta K_{T_{2g}} \frac{[2-(e^b+e^{-b})]}{e^b+e^{-b}+2}$	$\Delta K_{T_{2g}}$
$+\frac{\Delta K_{T_{2g}}}{2} \frac{[2-(e^b+e^{-b})]}{e^b+e^{-b}+2}$	$-\frac{\Delta K_{T_{2g}}}{2}$
$-\Delta K_{Eg} \frac{[2(e^c+e^{-c})-(e^{2c}+e^{-2c})-2]}{e^{2c}+e^{-2c}+4(e^c+e^{-c})+2} - \frac{3}{2} \Delta K_{T_{2g}} \frac{[2-(e^{2c}+e^{-2c})]}{e^{2c}+e^{-2c}+4(e^c+e^{-c})+2}$	$\Delta K_{Eg} + \frac{3}{2} \Delta K_{T_{2g}}$
$-\Delta K_{Eg} \frac{[2(e^c+e^{-c})-(e^{2c}+e^{-2c})-2]}{e^{2c}+e^{-2c}+4(e^c+e^{-c})+2} + \frac{3}{2} \Delta K_{T_{2g}} \frac{[2-(e^{2c}+e^{-2c})]}{e^{2c}+e^{-2c}+4(e^c+e^{-c})+2}$	$\Delta K_{Eg} - \frac{3}{2} \Delta K_{T_{2g}}$
$+2\Delta K_{Eg} \frac{[2(e^c+e^{-c})-(e^{2c}+e^{-2c})-2]}{e^{2c}+e^{-2c}+4(e^c+e^{-c})+2}$	$-2\Delta K_{Eg}$
with $\Delta K_{T_{2g}} = \frac{K_1 - K_2}{K_1 + K_2 + K_3}$	
$\Delta K_{Eg} = \frac{\frac{1}{2}(K_1 + K_2) - K_3}{K_1 + K_2 + K_3}$	

peculiar anisotropy is produced by the OH^- molecule itself, being affected only in a minor way by the change in dipole orientation from $\langle 100 \rangle$ to $\langle 110 \rangle$.

In the framework of the *crystal- and applied-field symmetries*, the two systems behave very differently. The $\langle 100 \rangle$ dipole system has a large $\Delta K(E_g)$ anisotropy producing maximum electro-dichroism under $\langle 100 \rangle$ fields and stress but zero $\Delta K(T_{2g})$ anisotropy, i.e., vanishing dichroism under $\langle 111 \rangle$ fields. The $\langle 110 \rangle$ system has a very small $\Delta K(E_g)$ anisotropy and therefore small di-

chroism under $\langle 100 \rangle$ field; the larger $\Delta K(T_{2g})$ anisotropy produces more sizable dichroism under $\langle 110 \rangle$ or $\langle 111 \rangle$ fields.

Similar as it was observed for the $\langle 110 \rangle \text{Ag}^+$ dipoles in RbBr and RbCl ,^{10,11} one can expect different rates for the reorientation of the $\Delta K(E_g)$ components (60° rotations) as compared to the reorientation of $\Delta K(T_{2g})$ components (90° rotation, see Fig. 5). Dynamic electrocaloric measurements² have shown a very fast ($\tau < 10^{-9}$ sec) relaxation behavior of OH^- dipoles in KI , which would make optical relaxation time measurements on this

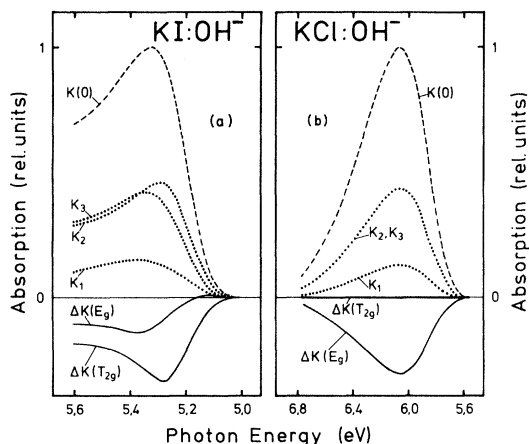


FIG. 8. Spectral shape of the optical anisotropy functions $\Delta K(E_g)$ and $\Delta K(T_{2g})$ in comparison to the OH^- absorption band $K(0)$ and its subcomponents K_1 , K_2 , and K_3 , (a) for the $\langle 110 \rangle$ dipole case ($\text{KI}:\text{OH}^-$) and (b) for the $\langle 100 \rangle$ dipole case ($\text{KCl}:\text{OH}^-$).

system extremely difficult or impossible.

Paraelectric resonance (PER) experiments on the $\text{KI}:\text{OH}^-$ systems⁵⁻⁷ agree with a $\langle 110 \rangle$ dipole model, but indicate as an anomaly the presence of a second multiplet of orientational states about 5 cm^{-1} above the ground-state multiplet. The dipole moment deduced from these PER studies for the lower multiplet of $p = 1.25e \text{ \AA}$ agrees rather well with our derived value of $1.35e \text{ \AA}$. The presence of the higher multiplet states (with a dipole moment of $p = 2.15e \text{ \AA}$) seems not to be detectable in our electro-optical measurements; this is reasonable, because at small fields the thermal population of these higher states is negligible at 2 K, while at high fields—where some effects may be expected—the electrochromism is saturated.

The only aberrations from a perfect model fit

are the spectral deviations of the observed $K(\omega)$ and $\Delta K(\omega)$ curves compared to the calculated ones observed under $\langle 111 \rangle$ field (Figs. 1 and 7). Obviously our assumption of “optically permanent” dipoles, which under field are only reoriented but not changed in their optical transitions, breaks down in this case. Particularly for E_{111} and perpendicular polarization, a field-induced shift of the band must be present too. One can be tempted to attribute this “anomaly” to the peculiarities of the $\text{KI}:\text{OH}^-$ systems, like its shallow orientational potential with $\langle 110 \rangle$ minima and/or the presence of the higher multiplet states. It should be pointed out, however, that the $\langle 100 \rangle$ -oriented OH^- systems have normally not been investigated^{1,2} as carefully as the $\text{KI}:\text{OH}^-$ system for possible field-induced spectral changes under E_{111} . In the only available short work where this was done (with ac modulation techniques),¹² a spectral shift effect under E_{111} and perpendicular polarization was observed in $\text{KCl}:\text{OH}^-$, very similar to the one in Fig. 7. It therefore appears that the simple—and highly successful—pure reorientation model has limitations for both the $\langle 100 \rangle$ and $\langle 110 \rangle$ dipole cases, which are worth being explored further experimentally and theoretically.

ACKNOWLEDGMENTS

The work of the University of Utah was supported by NSF Grants Nos. 77-12675 and 81-05332. One of us (S.K.) is grateful for the hospitality of the University of São Paulo, São Carlos Campus, Brazil, where part of the experimental work has been completed. This stay in São Carlos was made possible by the partial financial support by Finepe (Contract No. 32710BR).

*Present address: University of Osnabrück, Fachbereich Physik, 4500 Osnabrück, West Germany.

¹U. Kuhn and F. Lüty, *Solid State Commun.* **2**, 281 (1964).

²S. Kapphan and F. Lüty, *J. Phys. Chem. Solids* **34**, 969 (1973).

³D. G. Chae and B. G. Dick, *J. Phys. Chem. Solids* **34**, 1683 (1973).

⁴W. Heinicke and F. Lüty, *Bull. Am. Phys. Soc.* **17**, 143 (1972).

⁵F. Bridges, *Solid State Commun.* **13**, 1877 (1973).

⁶R. Hundhausen, R. Osswald, and H. C. Wolf, *Phys. Status Solidi B* **63**, 197 (1974).

⁷W. M. Kelly and F. Bridges, *Phys. Rev. B* **18**, 4606 (1978).

⁸S. Kapphan, in *Proceedings of the International Conference on Color Centers in Ionic Crystals, Japan, 1974* (Tohoku University, Sendai, Japan, 1974); *Verh. Dsch. Phys. Ges.* **9**, 587 (1974).

⁹R. Jimenez, S. Kapphan, and F. Lüty, in *Proceedings of the International Conference on Color Centers in Ionic Crystals* (University of Reading, Reading, England, 1971), Vol. 6; R. Jimenez and F. Lüty (unpublished).

¹⁰S. Kapphan and F. Lüty, *Phys. Rev. B* **6**, 1537 (1972).

¹¹R. Jimenez and F. Lüty, *Phys. Rev. B* **12**, 1531 (1975).

¹²A. Diaz Gongora and F. Lüty, *Phys. Status Solidi B* **85**, 693 (1978).

¹³R. Sittig, *Phys. Status Solidi* **21**, K175 (1967).